STATIC AND DYNAMIC BENDING STRENGTH OF THE LEG

P. Schreiber, J. Crandall
Department of Mechanical, Aerospace, and Nuclear Engineering
University of Virginia

T. Micek, S. Hurwitz
University of Virginia Department of Orthopaedic Surgery

G. S. Nusholtz
Chrysler Corporation

ABSTRACT

This study evaluates the relative contribution of axial compressive force and bending moment during static and dynamic loading of the tibia/fibula complex. The efficacy of the Tibia Index, the current standard for predicting leg injury, is also determined. Ten unembalmed cadaver legs were tested in quasi-static three-point bending, and twelve were subjected to dynamic three-point bending to compare static versus dynamic bending strength and energy to failure. Nine legs were subjected to dynamic three-point bending with a superimposed static axial compressive load. Legs were mounted with simple supports potted to the distal and proximal ends of the tibia/fibula complex, with the soft tissue structure maintained in tact. Impacts were delivered at mid-shaft, and directed posterioanteriorly. Load-cells measured forces delivered to the simple supports and impactor. High speed video recorded impactor displacement. Strain gauges mounted to the anterior and posterior tibia and fibula measured strain and strain rate at the outer-most fibers. CT scans provided cross-sectional properties of the bones along the axis of the leg. Dynamic bending exhibited a 69% higher breaking strength than legs subjected to quasi-static loading, with fractures showing a greater degree of comminution. In tests where a 4448N axial compressive load was superimposed upon a three-point bending load, the strength of the leg complex decreased by 17%. Axial compression appears to increase the bending moment in the tibia due to the curvature of the bone.

QUASI-STATIC THREE-POINT bending tests have been reported extensively throughout the literature as a means of determining the bending strength of the tibia. Most tests have involved denuded tibias loaded anterioposteriorly at the mid-diaphysis. Quasi-static tests are not ideal for predicting leg injury tolerance levels, because they ignore the viscoelastic properties of bone. Typically, bone demonstrates an increase in strength and stiffness at higher strain rate during dynamic loading (Martens et al, 1980, Mather, 1968). Carter (1977) reports that the modulus of elasticity and the ultimate strength of bone are proportional to the strain rate raised to the 0.06 power. Dynamic three-point bending tests have been performed by Mather (1968) and Nyquist (Nyquist et al., 1985). Mather's study used weighted impactors of varying mass to determine the impact energy to fracture half of the tested tibias. Bending moments at failure were not recorded. Energy values were determined from the kinetic energy of the impactor prior to fracture. Nyquist's dynamic bending tests loaded legs in the anterioposterior and lateromedial directions, keeping the soft tissue and fibula in tact. Nyquist's reported maximum moment for dynamic failure is questionable because he reports an estimated attenuation of peak force values by approximately 10%, due to a 100 Hz filtering process. No energy to failure values were determined in this study.

The axial compressive strength of the tibia and fibula has been reported by Messerer (1880) and Yamada (1970). Messerer's threshold values are approximately 1/3 of those reported by Yamada. This discrepancy may be due to the fact that Yamada tested short mid-diaphysis tibia segments, while Messerer compressed whole tibias. Bending, induced by the natural curvature of the tibia may have been a contributing factor to the lower threshold values reported by Messerer. The mid-diaphysis is also stronger in compression than the distal third region, which has a smaller cross-sectional area. Mean threshold values from these studies are summarized in Table 1 below.

Table 1. Summary of tibia threshold values reported in the literature

Maximum Average Bending Moment at Failure		
Messerer (in Nyquist 1986)	207 Nm Male 124 Nm Female	Quasi-Static, 3-Point Bending
Yamada (1970)	184 Nm Male/Female	Quasi-Static, 3-Point Bending
Weber (in Nyquist 1986)	165 Nm Male 125 Nm Female	Quasi-Static, 3-Point Bending
Nyquist (1985)	320 Nm Male 280 Nm Female	Dynamic, 3-Point Bending
Energy to Failure in Bending		
Mather (1968)	78.6 J Male 63.1 J Female	Dynamic, 3-Point Bending, Energy required to fracture half of specimens tested.
Mather (1967)	24.7 J Male/Female	Static 3-Pt Bending, Strain Energy Calculation
Martens (1980)	36.8 J Male/Female	Static 3-Pt Bending, Strain Energy Calculation
Tibia Maximum Axial Compressive Load		
Messerer (in Nyquist 1986)	10.36 kN Male 7.49 kN Female	Quasi-Static Compression of Whole Tibias
Yamada (1970)	32.95 kN Male 27.65 kN Female	Quasi-static compression of Mid-diaphysis Tibia Sections

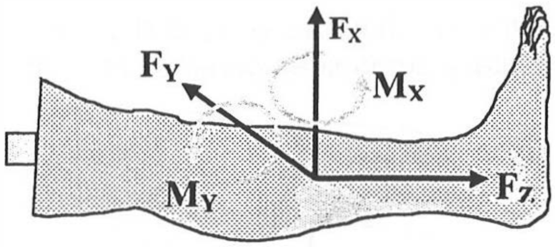

Figure 1. Force and Bending Moment Convention.

The Tibia Index (*TI*) is the injury tolerance criterion for combined axial and compressive dynamic loading of the leg as measured by Hybrid III tibial load-cells (Mertz, 1993). The *TI* is given by

$$TI = \frac{F}{F_C} + \frac{M}{M_C} < 1.0 \qquad F < 8\ kN \qquad (1)$$

where *F* is the measured compressive axial force (kN) in the *Z* direction (Figure 1). *M* was originally the measured bending moment in the *Y* direction (Nm), but was later revised to $M = \sqrt{M_X^{\ 2} + M_Y^{\ 2}}$, the measured resultant tibia moment in *X* and *Y*. M_C and F_C assume the following values:

	Small female	Midsize male	Large male
M_C = Critical bending moment	115 Nm	225 Nm	307 Nm
F_C = Critical compressive force	22.9 kN	35.9 kN	44.2 kN

A *TI* of 1.0 or greater exceeds the injury threshold. A modified *TI* threshold of 1.3 is currently in use by the EEVC (Hobbs, 1997). The *TI* has an additional constraint limiting the *Z* compressive load to 8 kN, which is twice the load required to fracture either the medial or lateral aspects of the tibial plateau or femoral condyles (Hirsch, 1965). The magnitudes of M_C and F_C are based on values published by Yamada (1970), obtained from quasi-static three-point bending and axial compression tests. The magnitude of the critical compressive force is based on localized failure of the tibia mid-diaphysis in tests involving short sections of bone compressed longitudinally.

The *TI* resembles an interaction formula for eccentrically loaded columns (Beer and Johnston, 1992). The local stress due to combined axial and bending loads for a beam with cross-sectional area A and moment of inertia I is given by

$$\sigma_{COMPRESSIVE} = \frac{F}{A} \pm \frac{Mc}{I} \qquad (2)$$

(combined compressive stress) = (centric stress) ± (bending stress)

where the sign of the bending stress term is negative on the tensile side of the beam, and positive on the compressive side (Figure 2). This combined loading results in reduced tensile stresses on the convex side of the beam and increased compressive stress on the concave side. Equation (2) may be transformed into a beam failure criterion by changing $\sigma_{COMPRESSIVE}$ to $\sigma_{CRITICAL}$, replacing the equality with an inequality, and rearranging terms, giving

$$\frac{F}{A\,\sigma_{CRITICAL}} \pm \frac{M}{\frac{I}{c}\sigma_{CRITICAL}} < 1 \qquad (3)$$

This equation resembles the *TI*, where $A\,\sigma_{CRITICAL}$ and $(I/c)\,\sigma_{CRITICAL}$ have been replaced by the experimentally determined parameters F_C and M_C.

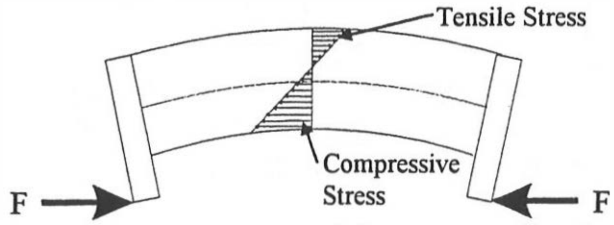

Figure 2. Stresses due to eccentric axial compressive loading of a beam.

Several assumptions regarding tibia fractures are inherent in the *TI*. The formulation assumes that failure occurs in compression. However, cortical bone is approximately 45% stronger in compression than in tension (Mow and Hayes, 1991). A clinical evaluation of automobile induced tibia fracture patterns conducted by the Department of Orthopaedic Surgery at the University of Virginia suggests tensile bending as a likely mode of failure (Micek, 1997). Another assumption is that the Hybrid III leg accurately measures the mid-shaft bending moment that would occur in the human tibia during axial compression of the leg. The structural geometry of the Hybrid III leg and the alignment of the leg shaft with respect to the joint centers is not exact to the human tibia/fibula. The magnitude of F_C is based on threshold values for tibia mid-diaphysis bone segments. However, the distal third region of the tibia possesses the smallest cross-section, and thinnest cortex, and would be more susceptible to failure in compression.

The study presented in this paper evaluates the bending strength of the leg (tibia-fibula complex with soft tissue in tact) by loading specimens in quasi-static and dynamic three-point bending. Unlike previous studies, loading was directed posterioanteriorly rather than anterioposteriorly at mid-diaphysis. This direction of bending was chosen based on a clinical evaluation of automobile induced tibia fracture patterns (Micek, 1997), and to simulate bending moments typically seen in the tibia during cadaveric and dummy automobile crash simulations performed at the UVA Automobile Safety Lab. This direction of bending is likely the result of two contributing factors in automobile accidents. The tibia is curved, bowing anteriorly at mid-diaphysis. Compressive loading of the leg, common in frontal collisions, will induce bending in the tibia such that the anterior aspect of the bone is placed in tension. Also typical in frontal collision is the tendency for the knee to contact the knee bolster while the foot is restrained by the toepan. When the leg is constrained in this manner, a bending moment is induced in the tibia and fibula due to inertial loading of the leg. While smaller than the compressive contribution, this direction of bending also places the anterior aspect of the bones in tension.

In evaluating the effects of an axial compressive load superimposed on a bending load, two possible contributions to the localized mid-diaphysis stress profile must be considered. Bone fails at a lower ultimate stress in tension than in compression. Axial compression will increase the anterior tibia tensile stress due to bone curvature, but will decrease the tensile stress by altering the mid-diaphysis cross-sectional stress profile. The relative contribution of each of these effects depends on bone geometry and magnitude of loads. Assessment of these factors and their contribution to bone fracture is difficult to estimate, requiring experimental investigation. The role of the fibula and soft tissue in supporting this structure may be significant, and have been left in tact for this study.

METHODOLOGY

Specimens were prepared by disarticulating the leg at the knee and ankle joint, and removing enough soft tissue to expose 70 mm of bone at the distal and proximal ends. The exposed ends were potted in PC-7 epoxy putty to a depth of 50 mm using removable molds. Simple support fixtures were attached to the hardened epoxy potting (Figure 3). Strain gauges (Micro-Measurements, model CEA-13-125UN-350) were adhered to the anterior surface of the bone at three locations: the mid-diaphysis of the tibia, the distal third of the tibia and the mid-diaphysis of the fibula. An additional strain gauge was added to the posterior mid-diaphysis of the tibia in tests where axial compressive loading was applied. Gauges were oriented to measure strain in the outermost fiber of the cross-section, along the longitudinal axis of the bones. Pre-test CT scans of each leg were obtained (5 mm contiguous slices) to determine bone cross-sectional properties and identify any pre-existing skeletal conditions. Bone properties were determined using a threshold Hounsfield unit of 1600 to distinguish cortical bone from cancellous bone and soft tissue. Cross-sectional areas and polar moments of inertia were calculated for each 5mm contiguous slice for both the tibia and combined tibia/fibula. Post-test radiographs (frontal and sagittal views) were taken and the leg dissected to evaluate test induced injury and classify fracture patterns.

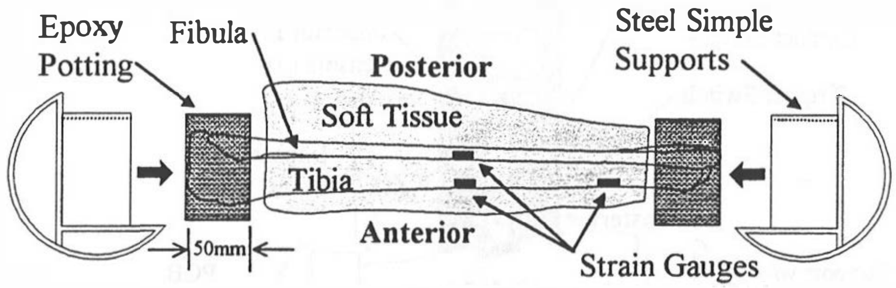

Figure 3. Specimen Preparation

Quasi-static three-point bending tests were performed using a Universal Test Machine (Tinius-Olsen, LoCAP 30,000). The leg and attached pivots were placed on a greased surface to minimize shear forces as the pivots rotated. Loading was applied to the posterior aspect of the leg, midway between the supports using a 25 mm diameter cylindrical contact surface aligned perpendicular to the bone. Loader displacement was directed posterioanteriorly at a rate of 25 mm/min, until both the tibia and fibula were fractured. Contact force and displacement were recorded for each test.

Dynamic three-point bending tests were performed using a 9.48 kg impactor released from a drop height of 2.85 m. The impactor was guided by a vertical linear bearing track as it fell and collided with the mid-diaphysis posterior aspect of the leg (Figure 4). Pre-impact velocity was 5.55 m/s, and remained within 60% of this value up to the instant of fracture. The impactor was brought to rest following fracture using a soft stop decelerator of crushable polystyrene. The proximal and distal simple supports each rested on greased plates. Each plate was supported by three quartz piezoelectric load sensors (PCB Piezotronics, model P212-B) aligned to measure force in the vertical direction. The load applied to each support was calculated by summing signals from the three load sensors. Impact load was measured using 3 piezoelectric load sensors mounted in a similar fashion between the impactor blade and impactor mass. Accelerometers mounted to the impactor blade allowed for inertial compensation of the impact load. The instant of impactor contact with the leg, t_0, was recorded by placing a conductive trigger switch on the leg at the region of impact. Data was sampled at a rate of 20,000 Hz, and filtered at SAE class 1000. High speed video (Kodak, model 1000-E, 1000 fps) recorded impactor displacement during the event.

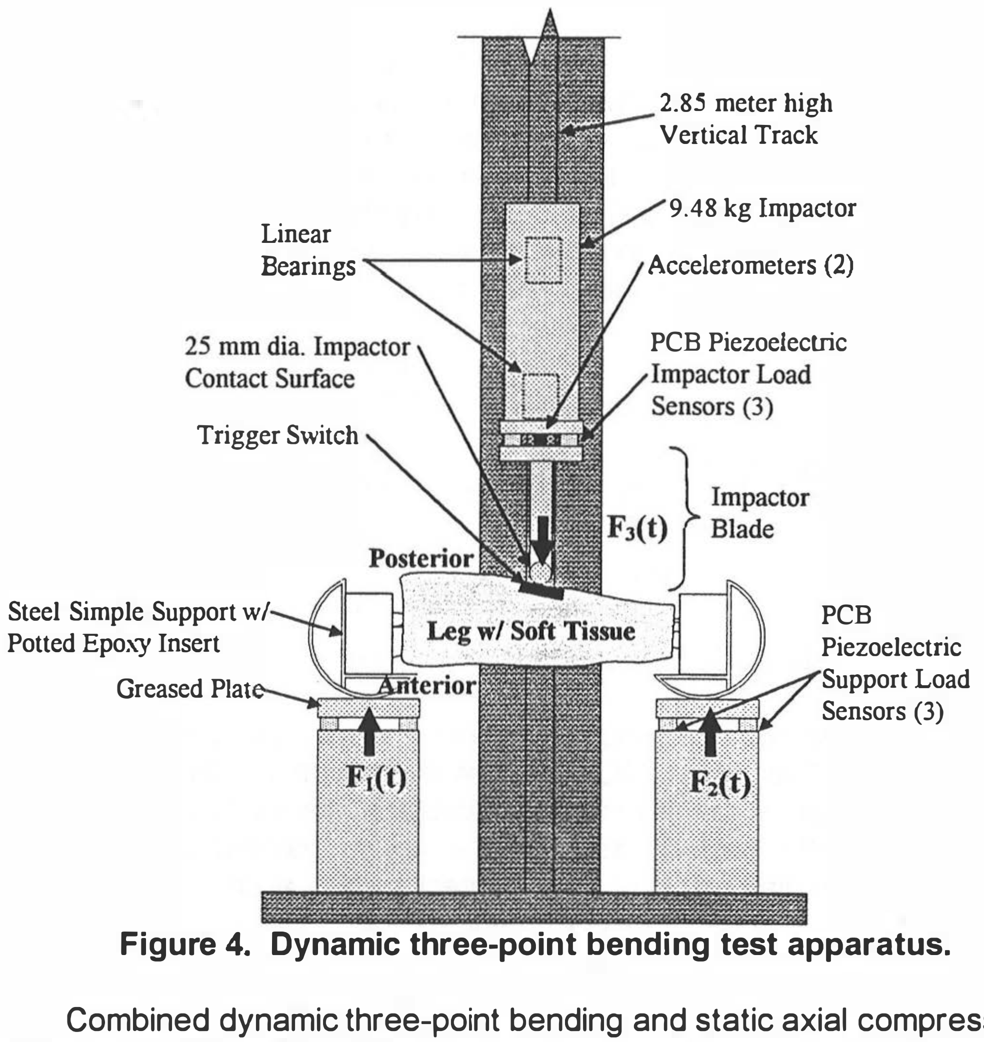

Figure 4. Dynamic three-point bending test apparatus.

Combined dynamic three-point bending and static axial compressive loading was achieved by adding a clamping mechanism to the dynamic test setup. The clamping mechanism consisted of roller bearings that transmitted a 4448 N compressive load to the simple supports (Figure 5). The bearings permitted the ends of the leg to rotate during bending. The load was maintained using two springs compressed by tightening nuts on threaded rods aligned with the leg on the medial and lateral sides. Two load-cells (AC Design, model 9503, 3000 lb) attached to the rods provided a measure of the compressive force during impact. The applied load remained within 10% of 4448 N until tibia fracture. Compressive loading was applied through the theoretical centers of pressure at the tibial plateau and tibial plafond (Fukubayashi, 1980, Ahmed, 1983, Brown et al., 1994). The tibial stem and the most proximal point of curvature of the tibial plafond were chosen as anatomical landmarks for locating the centers of pressure in the anterior-posterior direction. Locator screws in the epoxy potting molds were used to align these landmarks with the compressive loading vector. This alignment ensured that no "artificial" moments were produced when compressing the leg.

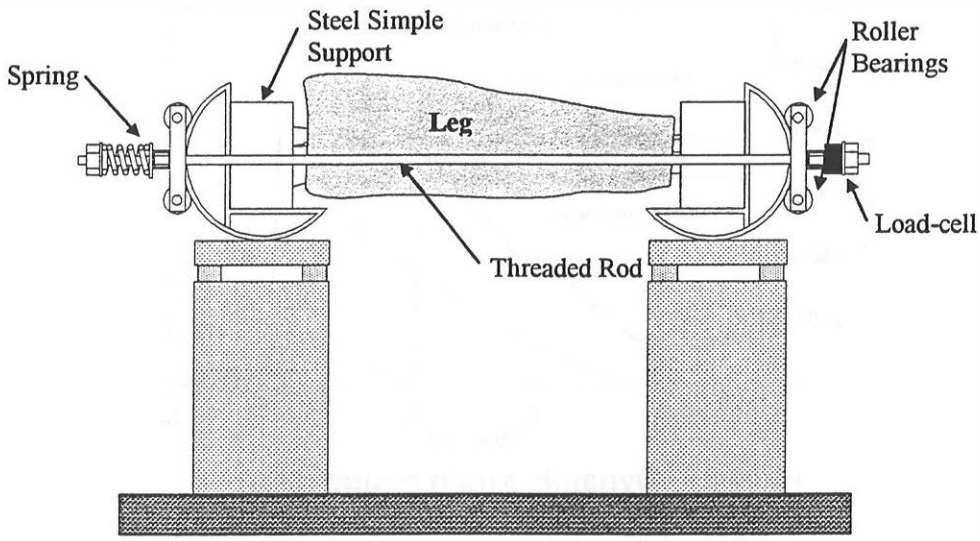

Figure 5. Clamping mechanism for applying axial compressive load.

For quasi-static tests, fracture of both the tibia and fibula was indicated by an audible crack accompanied by a 90% or more drop in load. The instants of fracture of the tibia and fibula were identified during dynamic tests using data from the strain gauges fixed to the anterior tibia and fibula. Figures 6 and 7 show typical plots of strain gauge data from quasi-static and dynamic bending tests, respectively, with the instant of fracture indicated by a sharp drop in strain. Fracture was proceeded by a small region of yielding in quasi-static tests, indicated by a slight decrease in the slope of the strain curve prior to drop-off. Strain rate in the outermost fibers near the fracture site was determined using the linear region of the strain curves for both quasi-static and dynamic tests. Because the fibula is situated posterior to the tibia at the region of impact, fibula fracture occurred before tibia fracture in all tests.

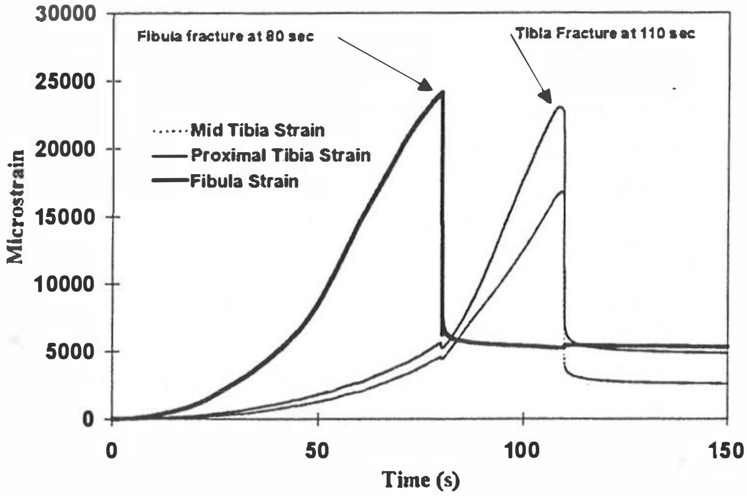

Figure 6. Quasi-static strain gauge data.

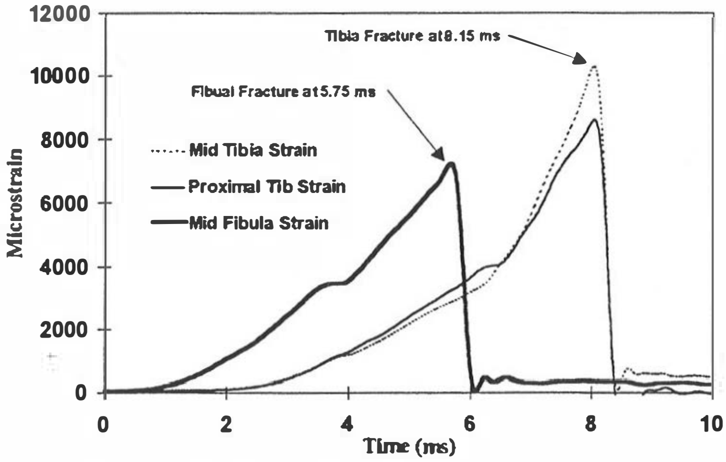

Figure 7. Dynamic strain gauge data.

ANALYSIS OF EXPERIMENTAL DATA

Maximum bending moment and energy to failure calculations were performed on all legs tested. Energy to failure for quasi-static tests was calculated as

$$E_{STATIC} = \int_{S_{CONTACT}}^{S_{FRACTURE}} F_{UTM}\, dS \tag{4}$$

where F_{UTM} is the force measured by the Universal Test Machine load-cell and dS is the differential loader displacement. $S_{CONTACT}$ and $S_{FRACTURE}$ denote impactor displacement at the instants of initial contact with the leg and complete fracture of the leg, respectively. Maximum bending moment was calculated as

$$M_{STATIC} = \frac{(F)_{MAX} \cdot L}{4} \tag{5}$$

where L is the distance between the simple supports. All bending moment calculations in this study are based on simple beam theory, and have ignored any higher order terms involving shear or large deflections at mid-shaft. These assumptions were felt to be valid, given that midshaft deflection during fracture was approximately 10 mm, while the diameter of the tibia is approximately 24 mm, and the distance between supports was approximately 350 mm.

Energy to failure and bending moment for dynamic three-point bending were calculated using the force as measured by the impactor load sensors. This load was inertially compensated using accelerometer data to account for the mass of the impactor blade (Figure 4). The inertially compensated impactor load, $F'_3(t)$ rather than two support loads, $F_1(t)$ and $F_2(t)$, was chosen for dynamic calculations because the support load signals were noisy following fibula fracture. This noise was attributed to the frequency response of the leg structure as the dynamic load was transmitted from the impactor through the leg to the supports. The peak impactor load and peak tibia strain occurred concurrently, whereas there was often a delay between peak tibia strain and peak support load. There was no evidence of oscillations in the impactor load signal due to the frequency response of the load sensors and impactor blade.

The dynamic bending moment at fracture was calculated as

$$M_{DYNAMIC\ BENDING} = (F_3')_{MAX} \cdot \frac{L}{4} \tag{6}$$

where F'_3 is the peak impactor load and L is the distance between supports. Dynamic bending energy to failure was calculated as

$$E_{DYNAMIC\ BENDING}(t) = \int_{S_{CONTACT}}^{S_{FRACTURE}} (F_3')\, dS \tag{7}$$

where dS is the differential displacement of the impactor, $S_{CONTACT}$ is the impactor displacement as it first contacts the leg, and $S_{FRACTURE}$ is the impactor displacement at the instant of tibia fracture, as indicated by strain gauge data.

For tests incorporating a static axial compressive load, the additional energy introduced to the leg by the compressive force was measured for each leg prior to destructive testing. The leg and attached pivots were compressed axially by the roller bearings at a rate of 5mm/min using a Universal Test Machine, while force versus displacement data were recorded up to the intended load of 4448 N. Axial compression energy was calculated as

$$E_{AXIAL\ COMPRESSION}(t) = \int_{S_0}^{S_{448N}} F_{UTM}\, dS_{UTM} \tag{8}$$

where F_{UTM} and dS_{UTM} are the force and differential displacement measured by the Universal Test Machine, respectively.

EXPERIMENTAL RESULTS

Results from the quasi-static bending, dynamic bending and dynamic bending with static axial compression are summarized in Tables 2, 3 and 4, respectively. Fractures have been classified according to fracture pattern and degree of comminution (Johner, 1983). Energy to failure, maximum bending moment and *TI* have been calculated for all tests. The critical values of F_C = 22.9 kN and M_C = 115 Nm, appropriate for 5th percentile females, were used to calculate the *TI* for all female specimens. The mean mass of tested female legs was 1.81 kg. The mean age was 57. The leg mass for 5th and 50th percentile females are 2.16 kg and 2.62 kg, respectively (McConville, 1978). *TI* calculations for male specimens used critical values for midsize males of F_C = 35.9kN and M_C = 225Nm.

For the ten legs tested in quasi-static three-point bending, the mean maximum bending moment was 241 Nm, the mean energy to failure was 59.2 J, and the mean *TI* was 1.85. The mean strain rate at mid-shaft was 440 microstrain/sec., with an average peak strain of approximately 2.5%.

In 40 % of the tests, tibia fractures occurred near the distal third, where the magnitude of the bending moment is approximately 67% lower than at mid-shaft. CT scans of the tibias indicate that the cross-sectional polar moment of inertia is 37% lower, on average, at the distal third than at mid-shaft, indicating that the bone is weaker in bending at the distal third region. CT scans also indicate that the combined tibia/fibula cross-sectional area is 27% lower, on average, at the distal third than at mid-shaft, indicating that the bone is weaker in compression at the distal third region.

Quasi-static bending moments obtained in this study were higher on average than values reported in all previous three-point bending studies in the literature. Several factors are possible contributors to this increased strength. Preserving the leg structure by keeping the fibula and soft tissue in-tact may have made the leg stronger in bending, although the influence of the fibula was minimized during quasi-static tests, where the fibula fractured before the maximum moment was reached. The posterioanterior direction of bending may provide a higher bending strength than the anterioposterior direction tested in previous studies. A pervious study by Yamada (1970), however, has reported similar tibia bending strengths in the anterioposterior and lateromedial directions.

Table 2. Quasi-static three-point bending test results

Leg	Energy to Failure (J)	Mid-shaft Moment (Nm)	*TI*	Age	Leg Mass (kg)	Sex	Fracture Classification	Fracture Location
63-L	47.0	144	1.25	34	1.81	F	A3-Transverse	Dist. 1/3
63-R	58.6	165	1.43	34	1.81	F	A3-Transverse	Dist. 1/3
58-L	69.4	264	2.30	51	1.93	F	A3-Transverse	Dist. 1/3
58-R	60.4	254	2.21	51	1.93	F	A3-Transverse	Dist. 1/3
59-L	44.4	252	2.19	45	1.59	F	B2- Butterfly	Mid-shaft
59-R	42.0	237	2.06	45	1.59	F	B2- Butterfly	Mid-shaft
52-L	49.9	256	2.23	64	2.03	F	A3-Transverse	Mid-shaft
52-R	46.9	257	2.23	64	2.03	F	B2- Butterfly	Mid-shaft
68-L	80.9	299	1.32	56	2.60	M	A3-Transverse	Mid-shaft
69-L	92.6	285	1.26	62	2.60	M	B2-Butterfly	Mid-shaft
Avg.	59.2	241	1.85	51	1.99			
St.Dev.	16.9	49	0.46	11	0.36			

For the twelve legs tested in dynamic three-point bending, the mean maximum bending moment was 408 Nm, the mean energy to failure was 68.6 J, and the mean *TI* was 2.76. The mean strain rate at mid-shaft was 4.24×10^6 microstrain/sec., with fracture of the tibia occurring around 1.00 % strain. In

79% of the dynamic tests, tibia fractures occurred at mid-shaft, beneath the point of impact, with fractures showing a higher degree of comminution than quasi-static fractures.

Comparing the results in Tables 2 and 3, an increase of 9.4 J between quasi-static tests and dynamic tests was not significant (p=0.174) based on a two sample T-test. This result is likely due to the high variance in samples (coefficient of variation of 28.7% and 38.6% for quasi-static and dynamic energy, respectively). An increase in dynamic bending moment over quasi-static bending moment of 167 $\pm$ 78 Nm (95% confidence interval, two sample T-test) was found to be significant (p<0.001). This corresponds to an expected increase in moment of 69.3 $\pm$ 32.5%. This increase in strength is likely a characteristic of the bone's viscoelastic response. Peak strain during dynamic bending was approximately 60% lower than quasi-static bending strain. The lower strain at fracture and higher degree of comminution associated with dynamic bending indicates that the bone acts stiffer and more brittle at higher strain rates, producing a higher force at fracture (Figure 8). The dynamically loaded bone absorbed a similar amount of energy as the quasi-static bone, while deflecting less. Dynamic energy is absorbed by the bone at a higher rate, and is dissipated through multiple crack formations near the region of impact, accompanied by a short duration spike in force (Figure 9). Results from Tables 2 and 3 agree with the relation between strength and strain rate reported by Carter (1977). The ratio of average quasi-static to dynamic bending moment is 241Nm/408Nm = 0.59. The ratio of quasi-static to dynamic strain rate raised to the 0.06 power is $(440/4.24\text{x}10^6)^{0.06} = 0.58$.

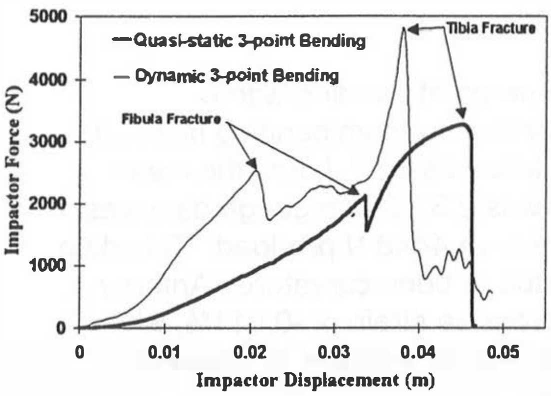

Figure 8. Quasi-static and dynamic force versus displacement.

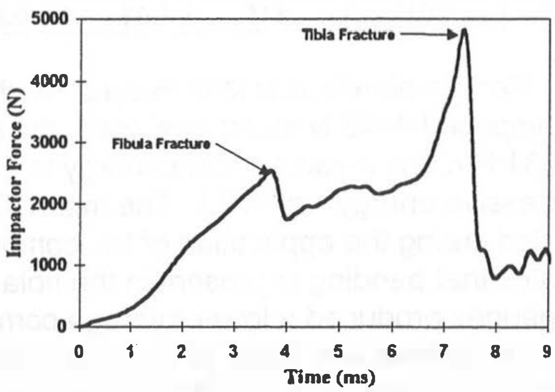

Figure 9. Dynamic Force versus time.

The dynamic frequency response of the leg may also contribute to the increase in stiffness and bending strength with dynamic loading. During quasi-static three-point bending, the leg assumes the fundamental mode shape, thereby producing a large deflection. As the impactor loading rate is increased, the leg will vibrate at a higher frequency, assuming a higher mode shape. This may produce a stiffer response, with stresses that are more localized beneath the impactor.

Two left/right matched pairs of legs (68-L/R and 69-L/R) were used to confirm the increase in bending strength and energy under dynamic loading. The left legs were tested quasi-statically and the right legs tested dynamically. Matched pairs showed an average 64% increase in bending moment and 37% increase in energy to failure for dynamic bending over static bending.

Table 3. Dynamic three-point bending test results

Leg	Energy to Failure (J)	Mid-shaft Moment (Nm)	*TI*	Age	Leg Mass (kg)	Sex	Fracture Location	Fracture Classification
48-L	32.4	239	1.06	83	1.80	M	Mid-shaft	A3-Transverse
1004-R	65.8	535	4.65	59	1.76	F	Mid-shaft	B3-Butterfly
1003-R	67.0	577	2.56	77	2.04	M	Mid-shaft	B3-Butterfly, Comminution
1000-R	77.6	458	2.04	85	3.08	M	Mid-shaft	B2-Butterfly
1005-R	57.9	445	3.87	75	2.16	M	Mid-shaft	B3-Comminution
1006-R	68.7	372	3.23	70	2.36	F	Mid-shaft	A2-Oblique,50% displaced
1002-R	55.1	259	2.25	70	1.70	F	Mid-shaft	B3-Butterfly, Comminution
1010-R	67.3	440	3.82	55	2.17	F	Mid-shaft	B3-Comminution
50-R	40.2	371	3.23	68	1.37	F	Distal 1/3	A3-Transverse
68-R	120.4	424	1.89	56	2.60	M	Mid & distal 1/3	C2-Segmental (2 fractures)
69-R	116.7	534	2.38	62	2.92	M	Mid & distal 1/3	B3-Butterfly (2 fractures)
73-L	54.17	242	2.11	61	1.54	F	Mid-shaft	B3-Butterfly
Avg.	68.6	408	2.76	68	2.13			
St.Dev.	28.5	115	1.02	10	0.54			

For the nine legs tested in dynamic three-point bending with a superimposed 4448 N static axial load, the mean maximum bending moment was 331 Nm, the mean bending energy to failure was 62.3 J, and the mean compressive energy was 4.7J. The mean *TI* was 2.3. Strain gauge data was recorded during the application of the compressive 4448 N pre-load. This data indicates that bending is present in the tibia due to bone curvature. Anterior tibia gauges produced a lower average compressive strain of -0.011%, while the posterior tibia and fibula gauges produced higher average compressive strains of -0.140% and -0.128%, respectively.

Seven matched left/right pairs of legs were split between dynamic bending tests with and without compression to facilitate assessment of the contribution of compressive loading to the bending strength. Test results were subject to a paired T-test analysis of variance to determine the statistical significance of a percent change in bending moment, energy, or *TI* with the application of the compressive load. Matched legs showed an average 19% decrease ($p<0.001$) in dynamic bending strength with the addition of the 4448 N compressive load. Bending energy increased by 9.8% ($p=0.088$). The *TI* decreased by 11.1% ($p=0.016$). The 11.1% decrease in the *TI* with the addition of the 4448N compressive load indicates that the axial compressive contribution in the *TI* formula is not weighted heavily enough, suggesting that the critical value for F_C is too large. If the *TI* is an accurate predictor of injury threshold, an increase in the measured compressive force *F* should be accompanied by an equivalent weighted decrease in the measured moment *M*, such that *TI* remains constant. Instead, we see a statistically significant decrease in *TI* with the addition of the axial load.

Quasi-static axial compressive loads were applied to the leg at a rate of 5mm/min to determine the compressive energy absorbed by the leg with the application of the 4448N load. During this preliminary procedure, two legs failed in compression at loads of 6220 N and 7410 N, with *TI* values at failure of 0.27 and 0.37, respectively. These legs provide another indication that the magnitude of F_C is too large, resulting in a *TI* that underestimates the compressive contribution to tibia fracture.

Table 4. Dynamic 3-point bending with axial compression test results

Leg	Axial Comp Enrgy (J)	Bend Enrgy to Failure (J)	Mid-shaft Moment (Nm)	*TI*	Age	Leg Mas (kg)	Sex	Fracture Location	Fracture Classification
1000-L	5.9	63.4	388	1.85	85	3.08	M	Mid-Tibia distal Fib	B2-Butterfly
1004-L	6.3	75.9	388	3.57	59	1.76	F	Prox-Tib. Prox & dist fib	A2-Oblique
50-L	3.7	51.9	319	2.97	68	1.37	F	Midshaft	A3-Transverse
1006-L	4.4	72.6	329	3.05	70	2.36	F	Mid-tibia. Prox, mid & dist fib	A3-Transverse
1003-L	3.9	80.7	482	2.27	77	2.04	M	Mid-tibia. Prox & dist fib	A3-Transverse
48-R	5.0	42.8	205	1.03	83	1.8	M	Mid-tibia. Prox & mid fibula	A3-Trans/oblique
73-R	4.5	58.7	213	2.05	61	1.52	F	Midshaft	B1-Butterfly
1001-L	3.9	45.3	212	1.07	94	1.73	M	Midshaft	B1-Butterfly
74-L	4.6	69.8	266	2.51	55	1.54	F	Mid-tibia. Prox & mid fib	B-3- Butterfly
Avg.	4.7	62.3	311	2.3	72	1.91			
St.Dev.	0.9	13.6	96	0.9	13	0.53			

CONCLUSIONS

There is a significant increase in stiffness and bending moment for legs tested in dynamic three-point bending, relative to legs tested in quasi-static three-point bending. Test results show an average increase in bending moments of 69% for legs tested dynamically over legs tested quasi-statically. Energy to failure values appeared consistent between dynamic and quasi-static tests.

Quasi-static bending moments obtained in this study were higher on average (254 Nm) than values reported in all previous three-point bending studies in the literature. Possible factors contributing to a higher observed bending strength in this study include preserving the fibula and soft tissue structure during bending tests, and changing the direction of loading to posterioanterior.

Axial compression of the leg under a 4448 N load produced lower compressive strain in the mid-diaphysis anterior tibia than in the posterior tibia and fibula. This difference in strain appears to be due to the eccentric loading that the mid-tibia receives during compression, due to the bone's natural curvature. The effective bending that the tibia receives during compression should be taken into account when analyzing data from anthropomorphic dummy tibia load-cells. The bending moment value measured by these load-cell can be easily corrected to account for compression induced bending in real legs.

The *TI* appears to underestimate the failure threshold of bones in both quasi-static and dynamic bending. In this study, mean *TI* values of 1.85 and 2.76 were obtained for quasi-static and dynamic bending tests, respectively. These results were obtained from an older specimen population. An increase in M_C, the critical bending moment, may be required to accommodate the increase in bone strength during dynamic loading. The *TI* appears to overestimate the failure threshold of bones loaded in compression.

The strength of the leg in both bending and axial compression is weakest at the distal third region. CT scans revealed that the cross-sectional moment of inertia and area are minimal in this region. Fracture of the tibia at the distal third occurred in 40% of legs tested quasi-statically, and in 21% of the legs tested dynamically. The distal third region of the leg, which is weaker in compression and bending, should be evaluated in determining M_C and F_C.

Further testing, involving quasi-static and dynamic axial compression of legs, is needed to asses a more appropriate value for F_C. The leg preparation described in this paper, which involved potting the ends of the bone, is felt to be inappropriate for axial compressive loads to failure. The potted ends showed evidence of failure at the bone/potting interface in preliminary axial compression tests. Future compressive testing should attempt to transfer loads via the ankle and knee joints. Axial loading of the leg through the knee and ankle joints will preserve the interaction of the proximal and distal tibio-fibular joints and guarantee that axial loading is transmitted biofidelically at the proximal and distal ends of the bone. Future testing will also assess whether buckling is a likely mode of failure when the leg is loaded in axial compression.

AKNOWLEGMENTS

This research was supported by The American Automobile Manufacturing Association. However, the analysis and conclusions contained in this paper are solely those of the authors, and have not been reviewed or approved by the sponsoring agency or other parties.

REFRENCES

Ahmed and Burke, J. Biomech. Engr., Vol. 105: 216-519, 1983.

Beer, F., Johnston, R., Mechanics of Materials, Second Edition, McGraw-Hill, 1992.

Brown, et al., Journal of Orthopaedic Trauma, 8 (6): 511-519

Carter, DR., Caler, WE, "Cycle-dependent and time-dependent bone fracture with repeated loading", J. Biomech. Eng, 105:166-170, 1983

Fukubayashi and Kurosawa, ACTA Orthopaedica Scandinavia, Vol. 51: 871-879, 1965

Hobbs, C., Gloyns, P., "European New Car Assessment Program (EURO-NCAP)". Version 1.0, January 1997, (Unpublished Project Report)

Hirsch, G. and Sullivan, L., "Experimental Knee Joint Fractures- A Preliminary Report.", ACTA Orthopaedica Scandinavia, Vol. 36, 1965.

Johner, R., Wruhs, O., Clinical Orthopaedics, 178:7-25 (Fig. 2), 1983

Martens, M., Van Audekercke, R., De Meester, P., Mulier, J. C., "The Mechanical Characteristics of the Long Bones of the Lower Extremity in Torsional Loading.", J. Biomechanics Vol. 13, pp. 667-676, 1980.

Martens, M., Van Audekercke, R., De Meester, P., Mulier, J. C., "Mechanical Behavior of Femoral Bones in Bending Loading.", J. Biomechanics Vol. 19, pp. 443-454, 1986.

Mather, Sherwood B., M.B., "Impact Tolerance of the Human Leg.", The Journal of Trauma, Vol. 8, No 6. 1968

Mather, Sherwood B., M.B., "Correlation Between Strength and Other Properties of Long Bones.", Journal of Trauma Vol. 7. No. 8, 1967

McConville, J., Laubach, L., Anthropomorphic Source Book, Volume I, NASA RP-1024, eds. W. Thornton and J. Jackson, 1978

Melvin, John W., Evand, F. Gaynor, "Extremities: Experimental Aspects", The Biomechanics of Trauma , Edited by Alan M. Nahum, and John W Melvin, Appleton- Century-Crofts/ Norwalk, Connecticut, 1985

Mertz, H., "Anthropomorphic Test Devices", Accidental Injury, Biomechanics and Prevention, edited by Nahum, A., Melvin, J., Springer-Verlag, 1993

Micek, T. *et al.*, "In-vitro tibial fracture fixation", UVA Dept. of Orthopaedics, 1997

Mow, V., Hayes, W., Basic Orthopaedic Biomechanics, Raven Press, New York, 1991

Nyquist, Gerald W., Cheng, R., El-Bohy, A., King, A. "Tibia Bending: Strength and Response." SAE #851728, 1985

Nyquist, Gerald W., "Injury Tolerance Characteristics of the Adult Human Lower Extremities Under Static and Dynamic Loading." Biomechanics and Medical Aspects of Lower Limb Injuries, SAE #861925, 1986

Yamada, H. Strength of Biological Materials, The Williams & Wilkens Co., Baltimore, 1970